Received: 11 September 2019 | Accepted: 22 November 2019

DOI: 10.1002/hyp.13661

RESEARCH ARTICLE

WILEY

Wetlandscape hydrologic dynamics driven by shallow groundwater and landscape topography

Leonardo E. Bertassello[1] | P. Suresh C. Rao[1,2] | James W. Jawitz[3] | Antoine F. Aubeneau[1] | Gianluca Botter[4]

[1]Lyles School of Civil Engineering, Purdue University, West Lafayette, Indiana, USA

[2]Agronomy Department, Purdue University, West Lafayette, Indiana, USA

[3]Soil and Water Sciences Department, University of Florida, Gainesville, Florida, USA

[4]Department of Civil, Architectural and Environmental Engineering, University of Padua, Padua, Italy

Correspondence
Leonardo E. Bertassello, Lyles School of Civil Engineering, Purdue University, West Lafayette, IN 47907-2051.
Email: lbertass@purdue.edu

Funding information
National Science Foundation, Grant/Award Numbers: 1354900, 1441188; Purdue University

Abstract

Wetlands play an important role in watershed eco-hydrology. The occurrence and distribution of wetlands in a landscape are affected by the surface topography and the hydro-climatic conditions. Here, we propose a minimalist probabilistic approach to describe the dynamic behaviour of wetlandscape attributes, including number of inundated wetlands and the statistical properties of wetland stage, surface area, perimeter, and storage volume. The method relies on two major assumptions: (a) wetland bottom hydrologic resistance is negligible; and (b) groundwater level is parallel to the mean terrain elevation. The approach links the number of *inundated* wetlands (depressions with water) to the distribution of wetland bottoms and divides, and the position of the shallow water table. We compared the wetlandscape attribute dynamics estimated from the probabilistic approach to those determined from a parsimonious hydrologic model for groundwater-dominated wetlands. We test the reliability of the assumptions of both models using data from six cypress dome wetlands in the Green Swamp Wildlife Management Area, Florida. The results of the hydrologic model for groundwater-dominated wetlands showed that the number of inundated wetlands has a unimodal dependence on the groundwater level, as predicted by the probabilistic approach. The proposed models provide a quantitative basis to understand the physical processes that drive the spatiotemporal hydrologic dynamics in wetlandscapes impacted by shallow groundwater fluctuations. Emergent patterns in wetlandscape hydrologic dynamics are of key importance not only for the conservation of water resources, but also for a wide range of eco-hydrological services provided by connectivity between wetlands and their surrounding uplands.

KEYWORDS

connectivity, DEM-analysis, groundwater-wetland interaction, landscape topography, wetlands, Wetlandscape hydrology

1 | INTRODUCTION

Wetlands are important eco-hydrological hubs (Uden, Hellman, Angeler, & Allen, 2014) that provide critical habitats for specialized fauna and flora (Mitsch & Gosselink, 2015; Werner, Skelly, Relyea, & Yurewicz, 2007), process nutrients (Cheng & Basu, 2017), and store water (Huang et al., 2011). Wetlands do not function in isolation but form an important component of the landscape mosaic of aquatic habitats (Mushet et al., 2019; Rains et al., 2016). Their persistent presence, diversity of habitats, and spatial distribution are important for diverse eco-hydrological functions they support (Cohen et al., 2016; Thorslund et al., 2017). Wetlands are dynamic and change in space

and time in response to unsteady external conditions (Shook, Pomeroy, Spence, & Boychuk, 2013; B. Zhang, Schwartz, & Liu, 2009), and to internal process feedbacks over the longer term (Tiner, 2016; Y. Zhang et al., 2012).

Duration and frequency of wetland inundation is among the most important factors affecting the biota they harbour (Werner et al., 2007). Wetlands often encompass a wide range of hydrologic conditions within a region (e.g., from shallow temporary ponds to deeper permanent water). This leads to a diversity of habitat types and quality, both within and among wetlands (Leibowitz, 2003). Understanding how landscapes with many embedded wetlands are constrained by landscape topography and respond to variability in hydroclimatic forcing informs ecological assessments of hydrological and ecological connectivity of wetland habitats and dispersal of aquatic fauna among wetlands at the regional scale. Ecological connectivity enables dispersal of organisms, while hydrologic connectivity is essential for flows of water and matter between landscape elements at multiple spatial and temporal scales (Peters et al., 2008; Tetzlaff et al., 2007). Thus, landscapes with numerous inundated wetlands sustain multiple landscape functions, such as flood attenuation, biogeochemical retention, refugia for semi-aquatic species, and dispersal of species among isolated aquatic habitats (Cohen et al., 2016; Rains et al., 2016; Smith, Tetzlaff, Gelbrecht, Kleine, & Soulsby, 2019).

Wetland hydrology at local scale is known to be affected by a variety of processes. Landscape attributes, such as topography, soils, bedrock permeability (Min, Paudel, & Jawitz, 2010), and temporal variation in climate, control the mode and magnitude of water fluxes (McLaughlin, Diamond, Quintero, Heffernan, & Cohen, 2019). While precipitation is known to be the main direct or indirect driver of stage variability, the presence of nearby waterbodies, such as rivers or lakes can affect wetland hydrological variability (Winter, 1999) and connectivity (Rains et al., 2016). In addition, wetland vegetation controls hydrologic conditions in many ways, including peat accumulation, shading (which affects water temperatures), and transpiration (Cronk & Fennessy, 2016). Here we seek to understand the occurrence and spatiotemporal distribution of numerous wetlands embedded within landscapes (hereafter *wetlandscapes*).

Identifying the spatiotemporal patters of inundated wetlands at landscape scales is challenging because wetland boundaries are dynamic in both space and time at multiple scales. Several methods have been proposed to identify wetlands using high-resolution images (Jaramillo et al., 2018; Montgomery, Hopkinson, Brisco, Patterson, & Rood, 2018; B. Zhang et al., 2009) or digital elevation models (Bertassello et al., 2018; Chu, 2017; Wu & Lane, 2017). Characterization of landscape surface topography is essential for wetland identification. Because water accumulates at low elevations, we expect that topography alone can reveal the locations of *potential wetlands*, defined here as the topographic depressions where water can accumulate. The U.S. Clean Water Act (Section 404) defines wetlands as "those areas that are inundated or saturated by surface or groundwater at frequency and duration sufficient to support […] a prevalence of vegetation, typically adapted for life in saturated soil conditions". The occurrence of inundated wetlands in a landscape with a specific topography depends on the underlying hydro-climatic conditions (Park, Botter, Jawitz, & Rao, 2014; Tamea, Muneepeerakul, Laio, Ridolfi, & Rodriguez-Iturbe, 2010). Hydro-climatic variability drives groundwater fluctuations, which play a key role in wetland hydrologic and vegetation dynamics (Bertassello, Rao, Park, Jawitz, & Botter, 2018; Min, Paudel, & Jawitz, 2010).

Here, we extended the parsimonious stochastic model for groundwater-dominated wetlands presented by Bertassello et al., (2018) from an analysis of single wetland dynamics to the entire landscape scale. To do this, we hypothesize that landscape topography and shallow groundwater dynamics control the hydrologic regimes of wetlandscapes. Based on this hypothesis, we assumed that the temporal fluctuations in wetland stage are surface expressions of the shallow groundwater. We consider the case when the groundwater level and wetland stage are in hydrologic equilibrium. In addition, we assumed that the shallow groundwater fluctuates following the mean elevation profile of the surface topography. Our model requires only two inputs: high-resolution digital elevation model (DEM) and measured or modelled temporal fluctuations in shallow groundwater level. Based on these two inputs, we present here a probabilistic approach to predict the long-term presence and persistence, as well as geometrical and hydrologic attributes of all groundwater-dominated wetlands embedded within a landscape. The proposed approach focuses on factors that dominate the emergence of landscape-scale spatial patterns despite local-scale heterogeneities.

We evaluated our model using data from the Green Swamp Wildlife Management Area (GSA) in southwest Florida. The GSA is a region of shallow groundwater overlying the highly permeable limestone of the Upper Floridan aquifer, favouring the exchange of water between wetlands and groundwater (Haag & Lee, 2010), consistent with our model assumptions. We used wetland stage and groundwater level data from 2010 to 2016 at six cypress domes within GSA. In addition, we used the National Wetland Inventory (NWI) (n.d.) (Tiner, 1997), to estimate the maximum number of inundated wetlands and their attributes. These observational data were compared with the model simulations.

In the following, we first present the details of how DEM data were used to estimate the distribution of all surface depressions where water accumulates (Sections 2.2 and 2.3). Estimation of the number of inundated wetlands and their hydrologic attributes are presented in Section 2.4. Salient features of the GSA case study site in Florida are presented in Section 3. We tested the reliability of assuming wetlands dynamics as entirely described by shallow groundwater fluctuations in Section 4.1. The estimated number of inundated wetlands (N_a) are described in Section 4.2, based on the intersection of shallow groundwater elevation, $z_{gw}(t)$, and the bottoms of surface depressions. Modelled temporal fluctuations and spatial patterns of wetland attributes (stage, area, perimeter, and volume) are shown in Section 4.3. We close in Section 5 with a discussion of the advantages, limitations, and applications of the modelling approach.

2 | METHODS

2.1 | Generalized model for groundwater-dominated wetlands

Starting from Bertassello, Rao, Park, et al. (2018), we conceptualize a wetland as a local depression in the landscape within which water can accumulate, with its bathymetry defined by the landscape topography (Figure 1a). When a sufficiently thick low-permeability layer occurs along the pool bottom, as a result of accretion of fine sediments or presence of confining unit, water exchange between wetland and shallow groundwater is governed by the wetted perimeter of the wetland bottom. As the hydrologic resistance of the wetland bottom approaches zero, the time-lag between wetland stage and the shallow groundwater diminishes, such that the wetland is simply a surface expression of shallow groundwater dynamics. In such cases, wetland stage and groundwater level are linked deterministically at all times, and the temporal variability of the wetland is entirely described by the dynamics of the shallow groundwater (Figure 1b). Thus, here we assume that the resistance of wetland bottom is close to zero and that the shallow groundwater is in equilibrium with wetland stage. The reliability of these assumptions has been supported at daily (Bertassello, Rao, Park, et al., 2018) and monthly (Nilsson, Rains, Lewis, & Trout, 2013) time scales. However, these assumptions may not be appropriate at smaller temporal scales (hours, minutes) because of slow hydrologic equilibration between wetlands and the shallow groundwater. Accordingly, in this paper, we focus on hydrologic variability at daily to monthly timescales.

We model water stage across a variety of wetlands in a geologically homogeneous domain by extending the model for groundwater-dominated wetlands proposed by Bertassello, Rao, Park, et al. (2018) from the analysis of a single wetland to a landscape comprising a large number of wetlands (>10 km^2). We assume that the regional shallow groundwater controls the hydrological dynamics in all the potential wetlands, defined as those landscape depressions where water can (temporarily) accumulate and that the hydrologic resistance of wetland bottoms is close to zero. In our analysis, the shallow groundwater table is assumed to be parallel to the local average elevation of the land surface (Figure 1c). The movement of groundwater is controlled to a large extent by land surface (Tóth, 1962; Winter, 1999), and variation in local topography affects the configuration of the water table (Sophocleous, 2002). The resulting groundwater flow pattern is also affected by the distribution of hydraulic conductivity in the soil. However, here, we assume an effectively homogeneous vadose zone to estimate the mean elevation in the groundwater, averaging local-scale variability.

The interactions of wetlands with shallow groundwater are governed by the position of the water bodies with respect to shallow groundwater (Winter, 1999). Indeed, our minimalist model prescribes that the number of inundated wetlands in a landscape depends on the interaction between landscape topography, defined by the elevation of wetland bottoms (z_B) and wetland divides (z_D), and the local position of the shallow groundwater (z_{gw}). In particular, as a byproduct of the assumed equilibrium between the shallow groundwater and the wetland stage, a given wetland is inundated when $z_{gw,\,i} > z_{B,\,i}$, while as the rising water table intersects wetland divide elevations, $z_{gw,\,i} > z_{D,\,i}$, two (or more) wetlands eventually begin to spill and merge, forming composite depressions (Wu & Lane, 2017). In the above notation, the subscript, *i*, is referred to the *i*-th wetland and the specific groundwater level position therein (Figure 1c).

The elevations of wetland bottoms and divides are results of the regional topography of the landscape, and thus can be derived from DEM data (Bertassello, Rao, Jawitz, et al., 2018; Le & Kumar, 2014). The procedure starts by evaluating the flow direction for each cell,

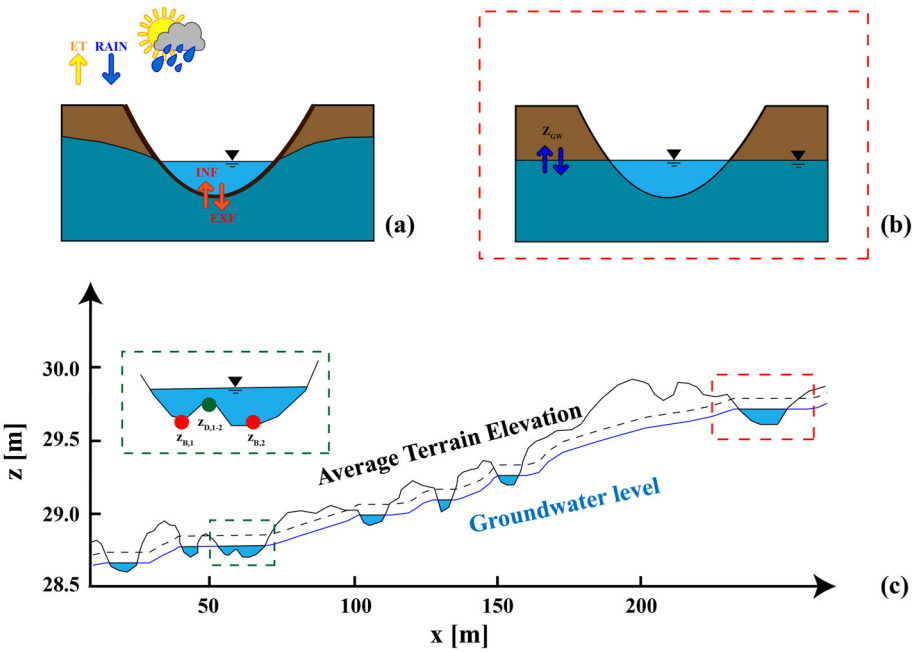

FIGURE 1 (a) Schematic conceptualization of the general hydrologic model proposed in Bertassello, Rao, Park, et al., 2018. Wetland dynamics are driven by hydroclimatic forcing (rainfall and evapotranspiration) and water exchange with shallow groundwater (infiltration and exfiltration). (b) Simplification of the general approach in the groundwater-dominated model. Here, the fluctuations of the groundwater are the only determinant for wetland hydrology. (c) Extension of the groundwater dominated model at landscape scale. The dashed line represents the average elevation of the terrain, while the continuous blue line is the shallow groundwater elevation, which is parallel to the mean slope of the elevation profile

and if the cell has no neighbours with lower elevation, it is identified as a sink, representing the bottom, z_B, of potential wetlands (N_p). The drainage basin of a potential wetland (wetlandshed) is the collection of cells from which water flows into a sink. To identify the divide for a wetland *i*, we need to consider an adjacent wetland *j*. The divide, z_D, between wetlands *i* and *j* is the lowest elevation of cells that are shared along the boundary of both wetlandsheds. If a wetland is bounded by more than one neighbour, more than one divide will be identified. In this case, the repetitions among the group of neighbouring wetlands are removed to assign each wetland to a single divide with another suitably identified wetland.

2.2 | Spatial detrending of landscape DEM

The main assumption of our approach is considering the shallow groundwater as parallel to the mean slope of the terrain. When the slope of the terrain is equal to zero, the shallow groundwater surface is a horizontal *xy*-plane that intersects the landscape topography at different levels (Osher & Fedkiw, 2001; Wu et al., 2019). In the general case, however, the groundwater table is not horizontal, an instance that makes the analytical description of the problem more complicated.

By applying a change of coordinates in the description of the system, we can simplify the problem and refer to a unique groundwater level, z_{gw}, across the entire domain. This is done by referring all the relevant elevations to the mean elevation of the terrain. Accordingly, the elevation of a given point, $z(x, y)$, in the original domain is transformed as:

$$z'(x, y) = z(x, y) - \langle z \rangle_{L\cdot L}(x, y) \tag{1}$$

where $\langle z \rangle_{L\cdot L}(x, y)$ is the moving average of the elevation profile for prescribed 2D windows of size ($L \times L$), centred in different positions along the *xy*-plane. Equation (1) is valid for the elevation of all the landscape points, including the wetland bottoms and divides. To keep the consistency of the formulation the groundwater level, z_{gw}, should be also shifted upward or downward of the same quantity in the transformed domain:

$$z'_{gw}(x, y, t) = z_{gw}(x, y, t) - \langle z \rangle_{L\cdot L}(x, y). \tag{2}$$

Note that z_{gw} is a function of time since it fluctuates in response to the hydroclimatic forcing. In the transformed spatial domain, the mean slope of the terrain is equal to zero ($\langle z'(x, y) \rangle = 0$); thus, $\langle z(x, y) \rangle$ and $\langle \langle z(x, y) \rangle + z'(x, y) \rangle$ are equal. Provided that the groundwater table is parallel to the mean slope of the terrain, the shallow groundwater level in the transformed domain, $z'_{gw}(x, y, t)$, must be uniform over the entire domain, and it results to be only a function of time: $z'(x, y, t) = z'_{gw}(t)$.

From Equations (1) and (2), the conditions for wetland inundation $z_{B,\,i} < z_{gw,\,i}$ and wetland merging $z_{D,\,i} < z_{gw,\,i}$ can be rewritten as:

$$z'_B(x, y) + \langle z \rangle_{L\cdot L}(x, y) < z'_{gw}(t) + \langle z \rangle_{L\cdot L}(x, y) \Leftrightarrow z'_B(x, y) < z'_{gw}(t) \tag{3}$$

$$z'_D(x, y) + \langle z \rangle_{L\cdot L}(x, y) < z'_{gw}(t) + \langle z \rangle_{L\cdot L}(x, y) \Leftrightarrow z'_D(x, y) < z'_{gw}(t) \tag{4}$$

This implies that the conditions for wetland merging and filling are the same also in the transformed domain, with the major advantage that in the transformed domain a unique (i.e., uniform) groundwater level can be used for all wetlands. For simplicity, in what follows, we refer to the detrended landscape using the variables z_B and z_D for wetland bottom and divide elevation, and a uniform horizontal shallow groundwater, z_{gw}.

2.3 | Probabilistic approach for identifying wetland occurrence

Evaluating the changes in the number of wetlands inundated, N_a, in a given landscape is of key importance for the multitude of ecohydrological functions they serve. The number of inundated wetlands, N_a, is affected by two main factors: the number of wetlands filled, and the number of wetlands merged. In particular, all those potential wetlands, N_p, whose bottom is lower than the shallow groundwater are considered as filled, while all those potential wetlands whose divide is lower than the shallow groundwater are considered as merged. The difference between these two quantities gives N_a. This number can be estimated from the distribution of wetland bottoms and divides, conceptualized here as two random variables. Accordingly, the cumulative distribution function (CDF) of the wetland bottoms (z_B) and wetland divides (z_D) relative to the mean local elevation (z'_B and z'_D in Section 2.1) is calculated. Then, the number of inundated wetlands can be obtained as $N_p \cdot P(z_B < z_{gw})$, while the number of merged wetlands is $N_p \cdot P(z_D < z_{gw})$. Finally, the difference between these CDFs represents the number of inundated wetlands for the given groundwater level, z_{gw}:

$$N_a = N_p[P(z_B < z_{gw}) - P(z_D < z_{gw})] \tag{5}$$

where $P(z_B < z_{gw})$ and $P(z_D < z_{gw})$ represent the CDFs of wetland bottoms and divides. Equation (5) accounts for the effect of the phenomena of filling and merging on the number of wetlands, triggered by groundwater fluctuations. Dividing Equation (5) by N_p, we obtain a normalized index, $f_{aw} = N_a/N_p$, which quantifies the fraction of potential wetlands that are inundated in the landscape. The probabilistic approach expressed in Equation (5) is a function of only the topographic characteristics of the landscape, represented here by the CDFs of wetland bottoms and divides. Thus, its applicability is not affected by the size of the spatial domain, but rather by the local heterogeneities of a given landscape (e.g., heterogeneity in wetland bottom permeability).

We identify three key threshold elevations, $z_{F,}$ $z_{C,\ and}$ z_M that define the dominant hydrological processes across the landscape

(Figure 2). In particular, z_F represents the initiation of filling based on the lowest elevation of wetland divides in the landscape, z_C is the critical groundwater elevation that maximizes f_{aw}, and z_M is the maximum elevation of wetland bottoms in the landscape. Based on Equation (5), the maximum value of f_{aw} is obtained when the difference between the z_B and z_D CDFs is largest. This critical groundwater level ($z_{gw} = z_C$) corresponds also to the intersection point between the probability density functions (PDFs) of wetland bottom and divide (Figure 2). These PDFs are obtained by computing the empirical distribution of wetland bottoms and divides.

When the groundwater level is below the wetland divides, $z_{gw} < z_F$, filling of landscape depressions is the dominant process; thus, the number of inundated wetlands increases because the groundwater level exceeds the elevation of potential wetland bottoms, z_B. In this phase, the merging process is prevented because the wetland divides are all higher than the groundwater stage. For higher groundwater levels, $z_F < z_{gw} < z_C$, the number of inundated wetlands is still increasing, but with a decreased rate due to the initiation of the merging process. The number of inundated wetlands in a given landscape is maximum when the groundwater reaches the elevation where the PDFs of wetland bottom and divide intersect (Figure 2d–f). This point represents a critical threshold for the landscape, which is determined only by morphological attributes. Above this limit ($z_C < z_{gw} < z_M$), the merging process overtakes the filling process, and the total number of inundated wetlands decreases as the water table rises. At this point, only potential wetlands at high elevations have not yet been filled. Finally, when $z_{gw} > z_M$ all the potential depressions are filled and only the effect of the merging process is observed.

The critical groundwater level corresponding to the maximum number of wetlands may or may not be reached depending on local hydrologic conditions. Three examples for the solution of Equation (5) using Gaussian PDFs for bottom and divide elevations are illustrated in Figure 2, and the parameters of these hypothetical distributions are reported in Supporting Information. In the example of Figure 2e,f, we observe that $f_{aw} < 1$ because the PDFs of wetland bottoms and divides are relatively close, such that the merging process begins before the filling of all potential depressions is completed. In contrast, when the PDFs of wetland bottoms and divides are farther apart (Figure 2d), the filling and merging processes are more separated and f_{aw} approaches 1 (Figure 2e) because all potential wetlands can be inundated before the merging process starts.

2.4 | Numerical model and estimation of wetland attributes

The probabilistic estimates of N_a from Equation (5) are compared with numerical integration obtained by censoring the landscape using a shallow groundwater table parallel to a horizontal *xy*-plane and counting the number of depressions below this level. This procedure is then repeated for several intersections of the shallow groundwater with the detrended topography. Note that the same considerations

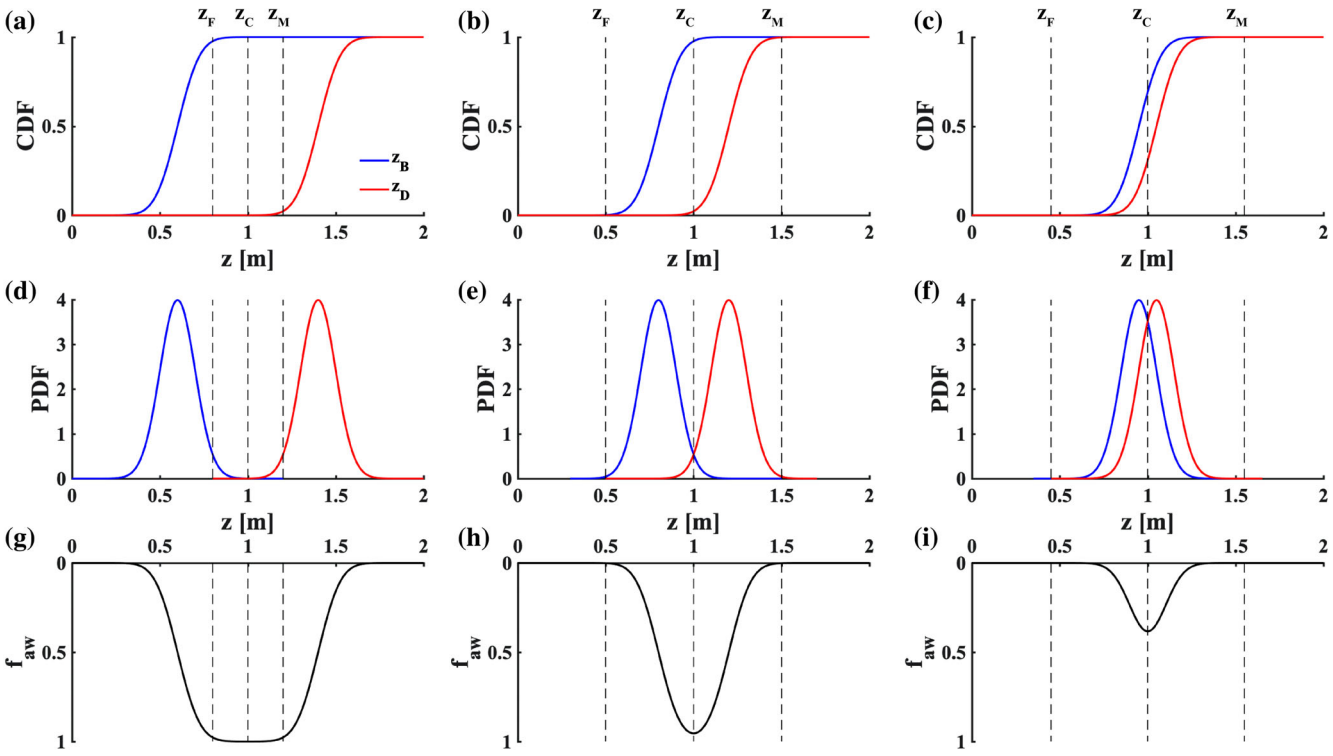

FIGURE 2 Hypothetical CDFs (a–c) and PDFs (d–f) of wetland bottom and divide. (g–i) Application of Equation (1) to estimate the number of inundated wetlands scaled to the total number of potential wetlands (f_{aw}). These three different conditions summarize how the fraction of inundated wetlands is influenced by the distribution of wetland bottom and divide. CDF, cumulative distribution function

are also valid for the original topography as stated by Equations (3) and (4), and thus by censoring the original topography using a shallow groundwater level parallel to the mean slope of the terrain.

This generalized model for wetland hydrology dominated by shallow groundwater (Figure 1c) allows for the estimation of wetland attributes in terms of stage, wetted-surface area, storage volume and wetted perimeter. These attributes vary as the shallow groundwater fluctuates in response to the hydroclimatic forcing. As the shallow groundwater level rises above wetland bottom, we calculate the stage (h) inside a given inundated wetland as the difference in elevation between the groundwater level (z_{gw}) level and the wetland bottom (z_B): $h = z_{gw} - z_B$. Following Chu, Zhang, Chi, and Yang (2010) and Le and Kumar (2014), wetland surface area, wetted perimeter, and storage volume are estimated for all wetlands at each groundwater level. The water-surface area of any wetland represents the maximum flooded surface area that can be observed in the wetland for a given z_{gw}. The surface area, $A_k^{(z_{gw})}$ [L^2], of the kth depression at that groundwater level, z_{gw}, is the sum of the areas of all individual cells within that depression. Wetland perimeter (P) is the sum of the distance between each adjoining pair of pixels around the border of the region. The storage volume (V) of any wetland is equal to its surface area, $A_k^{(z_{gw})}$, multiplied by the mean wetland stage computed by considering the difference between the groundwater level, z_{gw}, and the elevation, $z_{k,i}$ [L] of the i^{th} cell composing the inundated wetland.

Since the values of these attributes in the wetlandscape change as a function of $z_{gw}(t)$, we analysed the variation in the distribution of wetland stage, surface area, perimeter, and storage volume by computing their empirical complementary cumulative distribution functions (CCDFs) at different groundwater levels. We compared these empirical CCDFs with the theoretical trend prescribed by an exponentially tempered Pareto distribution $p(x) \propto x^{-b}e^{-cx}$. This type of distribution was chosen due to its flexibility in reproducing the tail behaviour dynamics and for investigating the emergent scale-free behaviour of wetland attributes (e.g., size distribution). In particular, the scaling exponent, b, of size distribution is generally related to the wetlandscape fractal dimension as $D = 2b$ (Russ, 1994; Seekell, Pace, Tranvik, & Verpoorter, 2013). This value is constrained between $D = 1$ (a population of smooth and circular objects) and $D = 2$ (a population of dissected objects). Thus, the fractal dimension, D, is a measure of the complexity of wetland geometry (Bertassello, Rao, Jawitz, et al., 2018).

3 | CASE STUDY AND DATA

3.1 | Green swamp area

The GSA covers ~450 km^2 in Hernando, Lake, Pasco, Polk, and Sumter Counties, FL. The GSA, a plateau above surrounding areas, is an important physiographic feature of Florida. We consider a 10 km × 10 km portion of the GSA (Figure 3). The area is not a continuous expanse of swamp but is a composite of many wetlands that are distributed uniformly across the area. Interspersed among the wetlands are low ridges, hills, and flatlands (Pride, Meyer, & Cherry, 1961). There is little development of the groundwater resource in this area, and surface-water levels are largely unaffected by human activities (Haag & Lee, 2010). Wetlands cover about one-third of the GSA, and much of the remainder is covered in natural pine flatwoods. Most of these wetlands are denoted as cypress domes since they contain large central trees tapering outward to smaller edge trees, a pattern often attributed to the fact that the underlying depressions are outward expanding karst features, giving them the characteristic dome appearance (Ewel, 1990; Powell, Wynn, Rains, Stewart, & Emery, 2019). Cypress domes are geographically isolated, freshwater wetlands occurring frequently in poorly drained, depressional areas within pine flatwoods uplands (Ewel, 1990).

The elevation of the land surface ranges from 25 to 55 m above mean sea level, thus the mean slope of the GSA is around 1 m/km (0.1%). In the GSA, the groundwater remains near the land surface for extended periods because of the hydrogeologic characteristics of the area. The GSA is underlain by several hundred feet of limestone and dolomite that have been periodically exposed to solution-weathering and erosion (Haag & Lee, 2010). The surface is mantled with a varying thickness of clastic material (sand and clay) that was deposited in fluctuating shallow seas (Lee, 2009). The Upper Floridan aquifer groundwater mound hinders the downward movement of water, as well as high clay content in the soils at larger depths and confining layers stabilize the groundwater (Nilsson et al., 2013; Spechler & Kroening, 2007).

3.2 | DEM data

The DEM represents a fundamental input for the groundwater-dominated model and the probabilistic approach defined in Equation (5). The DEM data is downloaded from the United States Geological Survey (USGS) platform National Map Viewer (n.d.) (https://viewer.nationalmap.gov) at 1/3 × 1/3 arc-sec resolution (~ 10 m × 10 m). The vertical resolution of the DEM data is 1.0 m. In addition to the primary domain, we also considered the DEM for three other domain sizes (3 km × 3 km, 5 km × 5 km, and 20 km × 20 km) to assess the reliability of the probabilistic approach over multiple spatial scales.

Before applying the probabilistic approach to assess the fraction of active wetlands as a function of the groundwater level, we detrended the slope of the terrain following Equation (1) by evaluating the moving average of the elevation profile for prescribed $L \times L$ windows. The chosen L value minimizes the differences between the number and the size distribution of wetlandsheds identified both from the original DEM and the detrended DEM. Here, the selected value of L = 1,000 m captures the original landscape topography without losing local information in terms of number of potential wetlands and their characteristics (see Supporting Information for details). Finally, we shifted this detrended DEM by adding the mean elevation of the region $\langle z \rangle$. Figure 3a,b illustrates the procedure of detrending in GSA. The change of coordinates from the original DEM (Figure 3a)

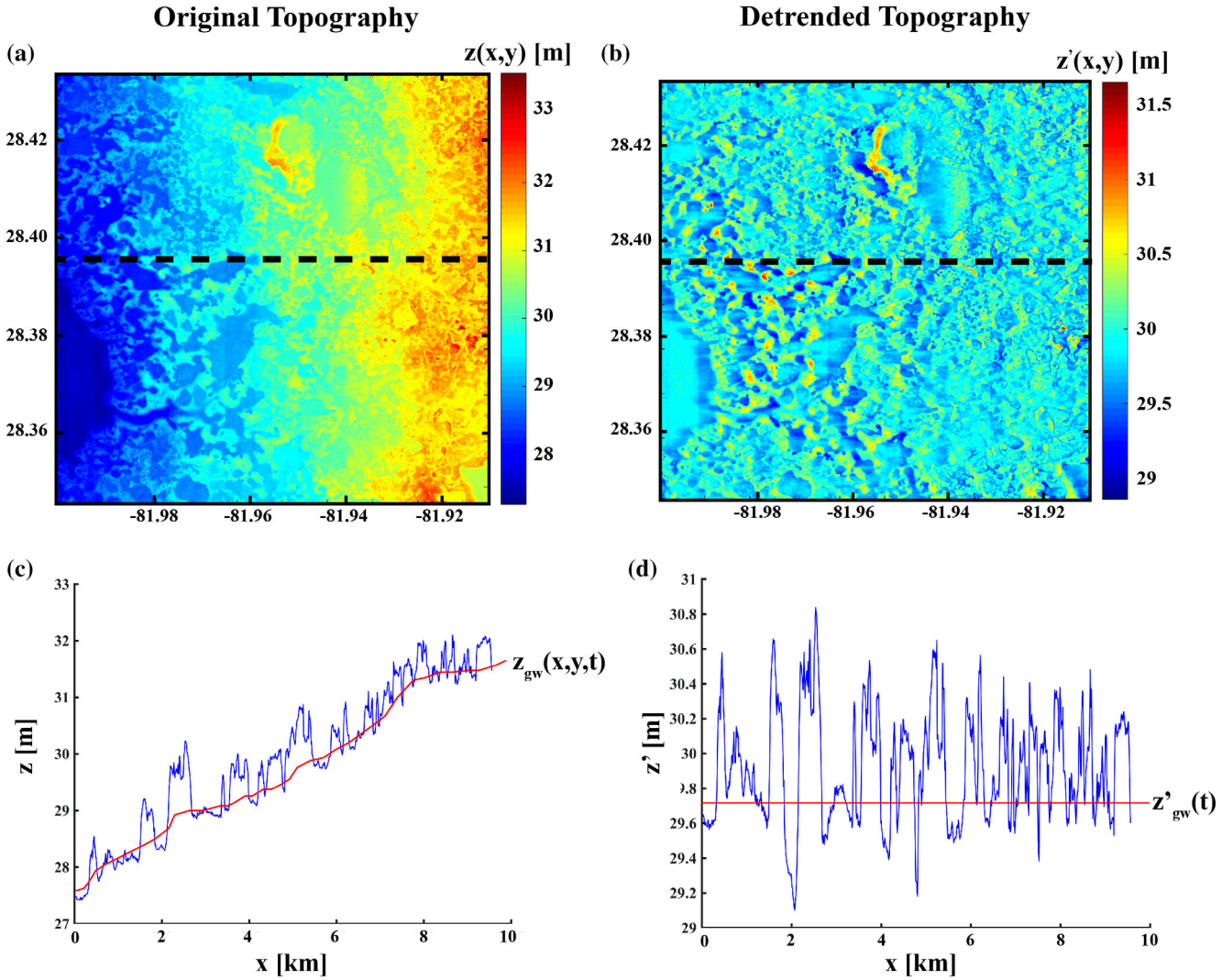

FIGURE 3 Comparison between the original (a) and detrended DEMs (b). The dashed line represents the elevation profile that is used as an example in (c) and (d), where we compare the landscape censored using a groundwater level that follows the original topography (c) and a horizontal groundwater level (d)

only produces a new DEM detrended from its regional topography (Figure 3b). We show that censoring the original topography using a shallow groundwater table that follows the mean elevation of the terrain (Figure 3c) is equivalent to censoring a detrended DEM using a horizontal groundwater table at the mean elevation of the landscape (Figure 3d). Indeed, the spatial distribution of wetland levels is the same in both cases. Furthermore, this result can be obtained for all groundwater levels parallel to the mean slope of the terrain (e.g., parallel to $z_{gw}(x, y, t)$ or $z'(t)$ in Figure 3c,d).

3.3 | Hydrologic data

The second key input for our model is the fluctuations of the shallow groundwater. The Southwest Florida Water Management District (SWFWMD) has established several long-term sites for monitoring groundwater provision and wetland protection in this region (Haag, Lee, & Herndon, 2005; Nilsson et al., 2013; Rochow & Lopez, 1984). We used wetland and groundwater data recorded at monthly resolution by SWFWMD for six cypress wetlands in the GSA (Figure 4). Two monitoring wells associated with each wetland were used. One monitoring well is located within the wetland close to a staff gauge, henceforth referred to as wetland well, and the other is in the nearby upland area surrounding the wetland, henceforth referred to as the upland well. The upland well data represent groundwater levels adjacent to the wetlands. Wetland and groundwater elevations were monitored over a period of 7 years, 1 January 2010 through 31 December 2016. Wetland bottoms for the six cypress domes were identified by the SWFWMD as the dry reading mark on the staff gauge and are assumed to represent the lowest point in the wetlands (Nilsson et al., 2013).

We also compared the maximum number of wetlands estimated by our model and those listed in the NWI database. The NWI database provides wetland data in terms of number and spatial extent

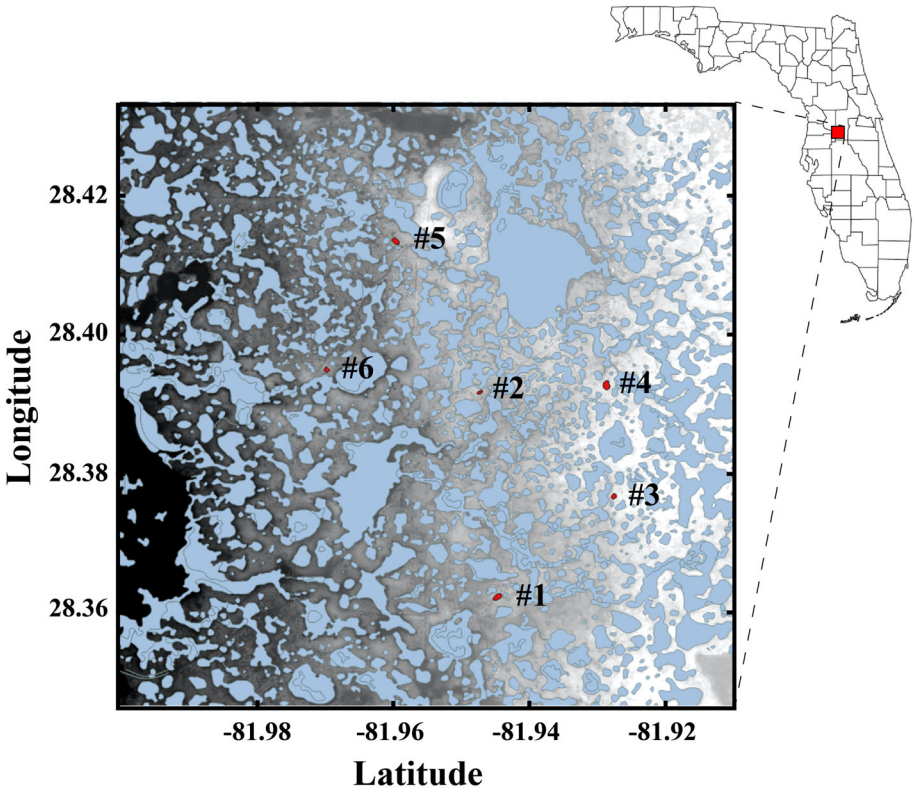

FIGURE 4 A 10 km × 10 km study area near Green Swamp, Florida. Approximately 1,300 wetlands are identified from the National Wetland Inventory (NWI) database (blue polygons). The six cypress wetlands considered in this study are highlighted in red and their identification number is reported

(area and perimeter). The NWI data are obtained from repeated photointerpretation of multiple aerial images (updated today by the US Fish and Wildlife Service at a rate of 2% per year), and despite the limitations (Tiner, 1997) these maps continue to be the most frequently requested source of wetland data in the USA for a variety of purposes. The data were downloaded from the NWI online platform (https://www.fws.gov/wetlands) and are characterized by the same spatial extent of the DEM (10 km × 10 km). We limited the number of inundated wetlands estimated by our model by the minimum size prescribed by the NWI in this region, which is 142 m^2. All wetlands smaller than this threshold are neglected. Indeed, these potential wetlands are likely to be associated with random error in the DEM (depressions ≤ 2 pixels).

4 | RESULTS

4.1 | Reliability of generalized wetland hydrology model

The main assumption of the model we proposed in Section 2.1 is that wetland stages are surface expressions of shallow groundwater level. We investigated the validity of this assumption by comparing the available hydrologic data in the six cypress wetlands.

The water levels monitored in the wetlands (w_i) and groundwater wells (gw_i) were strongly correlated, $\rho(w_i, gw_i) = 0.92 \pm 0.05$ for the six wetlands, indicating persistent coupling between wetland and groundwater dynamics. Therefore, an increase in the groundwater level is translated in an increased stage in all the six wetlands. Synchronous time series of wetland and groundwater level are compared in Figure 5. Both the time series are limited by the wetland bottom value, z_B, identified by the SWFWMD (Table 1).

We observed that for all the times when the shallow groundwater rises above wetland bottom ($z_{gw} > z_B$), the wetland is inundated, suggesting that wetland surface dynamics are strongly associated with the groundwater fluctuations, with mean absolute error (MAE) between observed wetland and groundwater data <20 cm in the six wetlands (Table 1). Observed discrepancies may be explained by lower-permeability sediment layers in the wetland bottoms that affect water exchange between the wetlands and the groundwater, or to the differences in specific yield between the wetland and the surrounding upland soils (Acharya, Jawitz, & Mylavarapu, 2012; Min, Paudel, & Jawitz, 2010), leading to standing water within the wetlands even if the groundwater level is below the wetland bottom. Since our purpose is not to assess the local hydrologic dynamics of each wetland, but, instead, to study how the interplay between shallow groundwater and regional topography lead to the occurrence and persistence of wetlands, our minimalistic approach does not include these local processes and heterogeneities. Overall, we observed that in 87% (± 0.07%) of the paired observations, wetland and groundwater show the same condition of inundation or dryness, suggesting that wetland dynamics are mainly driven by the fluctuations of the groundwater level.

4.2 | Application of the probabilistic approach to green swamp area

Although the six wetlands are located several kilometres apart, they exhibit similar hydrologic responses given shared regional rainfall

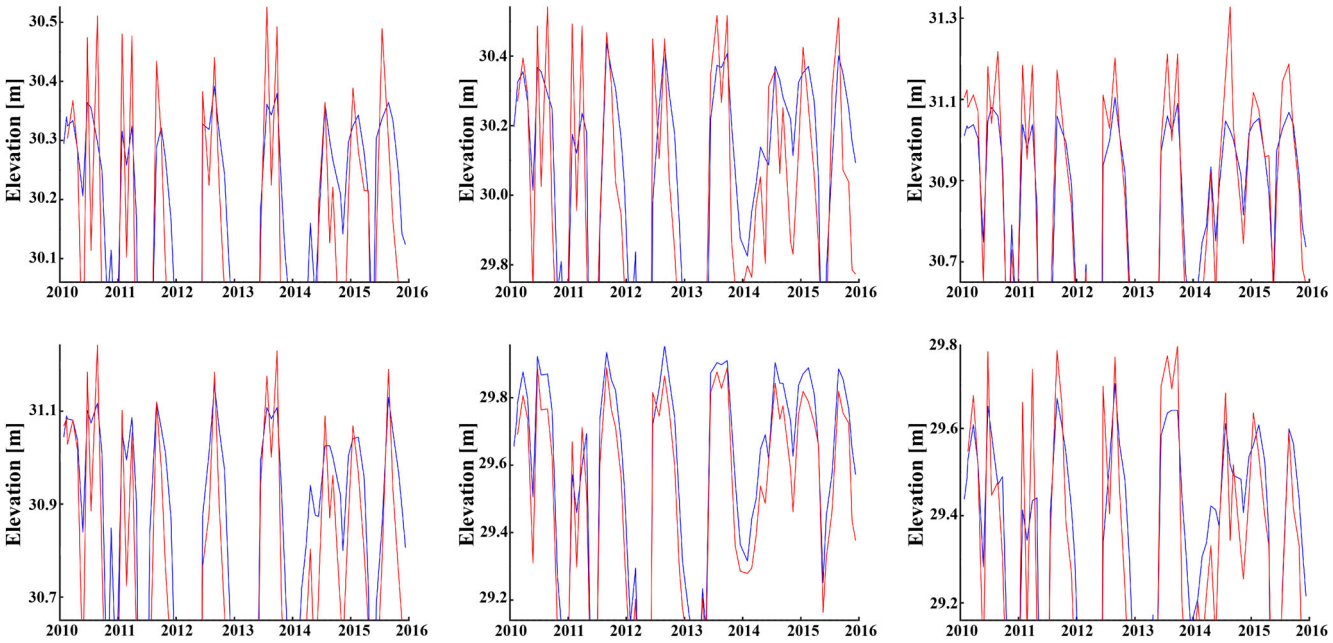

FIGURE 5 Comparison between the wetland stage (blue lines) and groundwater level (red lines) elevations from the six wetland-paired wells in the GSA. Note that the origin of *y*-axis is coincident with wetland bottom. GSA, Green Swamp Wildlife Management Area

TABLE 1 Statistics for the groundwater and the wetland level in the six wetland-paired wells

	GS #1	GS #2	GS #3	GS #4	GS #5	GS #6
$\rho(z_{gw}, z_{wet})$	0.89	0.84	0.95	0.93	0.98	0.92
MAE	0.17	0.20	0.08	0.16	0.10	0.15
z_B	30.06	29.75	30.65	30.65	29.14	29.16
Area ($\times 10^3$)	7.80	3.00	4.60	10.40	7.10	4.00

Note: We reported the correlation coefficient $\rho(z_{gw}, z_{wet})$ and the mean absolute error (MAE) between wetland and groundwater level. Wetland bottom and wetland area for the six cypress domes are obtained from the Southwest Florida Water Management District (SWFWMD). The unit of measurement of the MAE and wetland bottom is meter (m), except cypress domes area is in square meters (m^2), and the correlation coefficient is dimensionless.

patterns and shallow groundwater. This also suggests that patterns observed at these six wetlands may occur in numerous other wetlands in the same region. The results of the application of the Equation (5) to the slope-detrended landscape are reported in Figure 6a,b. The PDFs of wetland bottom and divide are similar, suggesting high correlation between the elevation points.

The relatively small differences in elevation of bottoms and divides in this landscape imply rapid merging of inundated depressions process as the groundwater rises. Thus, the peak value for f_{aw} is only 0.53%, because many of the small potential wetlands are merged in larger complexes that include more than one wetland bottom (z_B). The probabilistic approach (Figure 6b) shows good agreement (MAE = 90 wetlands) between the number of inundated wetlands estimated using Equation (5) and the numerical simulations obtained from slicing the DEM using a groundwater level that follows the mean slope of the region. In particular, the probabilistic approach tends to slightly overestimate the number of inundated wetlands during the merging process, while during the filling the MAE is close to zero.

The shape of the distribution describing the number of inundated wetlands is right-skewed unimodal, with a single peak representing the maximum number of inundated wetlands, close to 1,500 in this case. The actual number of inundated wetlands depends on the shallow groundwater fluctuations. Thus, in Figure 6b we reported also the PDF of the observed groundwater elevation z_{gw} (see Section 3.2 and Figure 5) detrended using Equation (2). The intersection between the PDF of z_{gw} and the distribution describing the number of inundated wetlands reveals how many wetlands could be inundated during the observation period. The groundwater PDF spans a large range of the inundated wetlands, suggesting that the maximum number of inundated wetlands can be reached, even though the mean of the groundwater PDF is at a lower elevation.

The probabilistic approach defined by Equation (5) was also tested in three other spatial domains within the GSA (Figure 6c). Two subsamples (3 km × 3 km and 5 km × 5 km) and a larger domain (20 km × 20 km) were used to assess whether the topographic characteristics (distribution of wetland bottoms and divides) are maintained

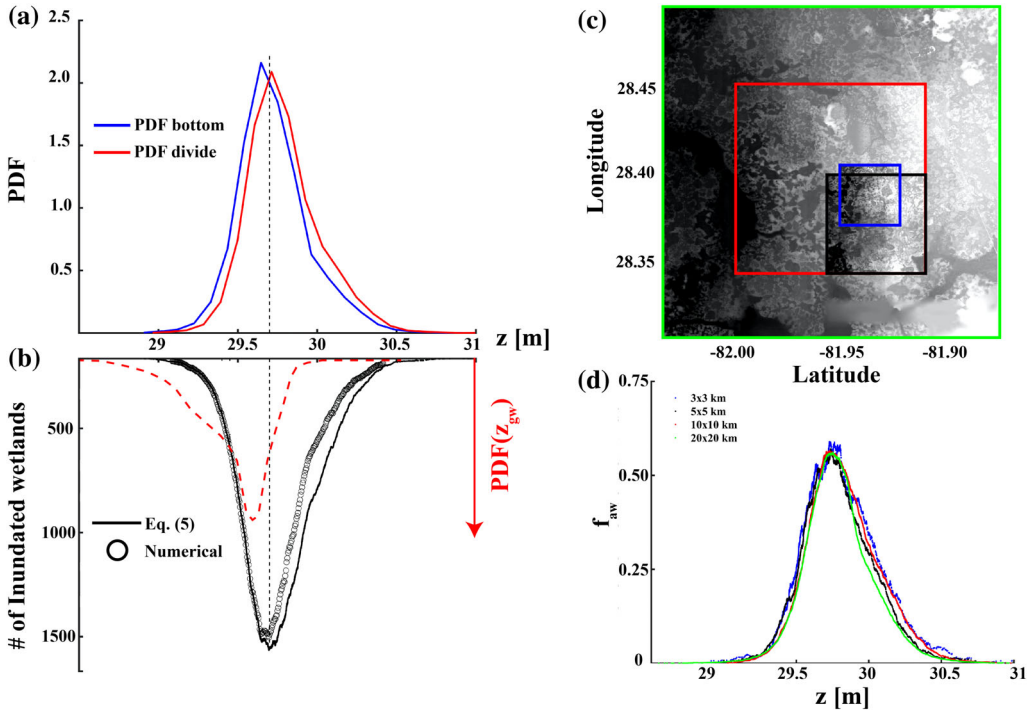

FIGURE 6 Application of the proposed model to the Green Swamp Area. (a) The results in terms of the PDFs for wetland bottom and divide. (b) The comparison between the number of wetlands estimated by the model and by the analytical approach provided in Equation (5). The red dashed line is the PDF of the water table obtained from the detrended empirical data. Extrapolation of the probabilistic approach across different domain sizes (c, d)

at different spatial scales. The 20 km × 20 km landscape covers almost the entire extent of the GSA. The inundated wetlands in all four spatial domains have equivalent topographic characteristics (Figure 6d). These results suggest that GSA is effectively homogeneous; local heterogeneities are not large enough to drive spatial variability within the four considered regions.

4.3 | Whole-landscape wetland hydrologic dynamics

The wetlandscape hydrologic dynamics were also analysed by comparing the distributions of estimated hydrologic attributes in terms of stage, surface area, storage volume and wetted perimeter (Section 2.3) at different groundwater levels for the entire 100 km^2 wetlandscape. The spatial dynamics of wetland attributes are shown in Figure 7 as CCDFs. As the groundwater level increases, we observe a progressive increase in the mean of such distributions since more landscape depressions fill. The distribution of wetland stage is described by an exponentially tempered Pareto distribution. Indeed, deviations from a Pareto distribution are evident both in the upper and lower tails. Alternative distributions, such as gamma (or lognormal) better describe the empirical pattern of wetland stage (see Supporting Information). Since rainfall input represents the main source of variability in the shallow groundwater and, therefore, for wetlandscape hydrologic dynamics, the CCDF of wetland stage is consistent with the (nearly) gamma-distributed steady-state distributions obtained in similar environmental systems (Botter, Basso, Rodriguez-Iturbe, & Rinaldo, 2013; Park et al., 2014; Porporato, Daly, & Rodriguez-Iturbe, 2004).

The CCDFs for wetland perimeter, surface area, and storage volume are described by an exponentially tempered Pareto distribution as well. In particular, these distributions vary as a function of changing hydrologic conditions. This tendency is manifested in the wide range for the tempering constant, c. The largest tempering occurs under dry conditions that constrain the shallow groundwater at lower levels. Under these conditions only a few small wetlands are water-filled and the mean of the CCDFs is shifted at lower values (red dashed lines in Figure 7). As the water table rises in response to incoming rainfall events, the tempering decreases and the number of larger wetlands increases, along with their hydrological attributes. The CCDFs become more heavy-tailed (black dashed lines in Figure 7) and their mean is shifted to larger values. When the simulated data are tempered, as we obtained during dry conditions for the shallow groundwater, non-Pareto distributions are indistinguishable from Pareto distributions (Seekell & Pace, 2011). Consequently, size, perimeter, and volume distributions may be described by alternative theoretical distributions (see Supporting Information for comparison with gamma and lognormal CCDFs) that mimic the trend of Pareto distribution for limited values of the considered variables.

Wetland size distributions reflect the wetlandscape hydrologic dynamics elucidated in our analyses of the observational data presented foregoing paragraphs. Shallow groundwater variability causes fluctuations in the tail of the CCDFs. The exponentially tempered Pareto distribution well reproduces this pattern and is consistent with

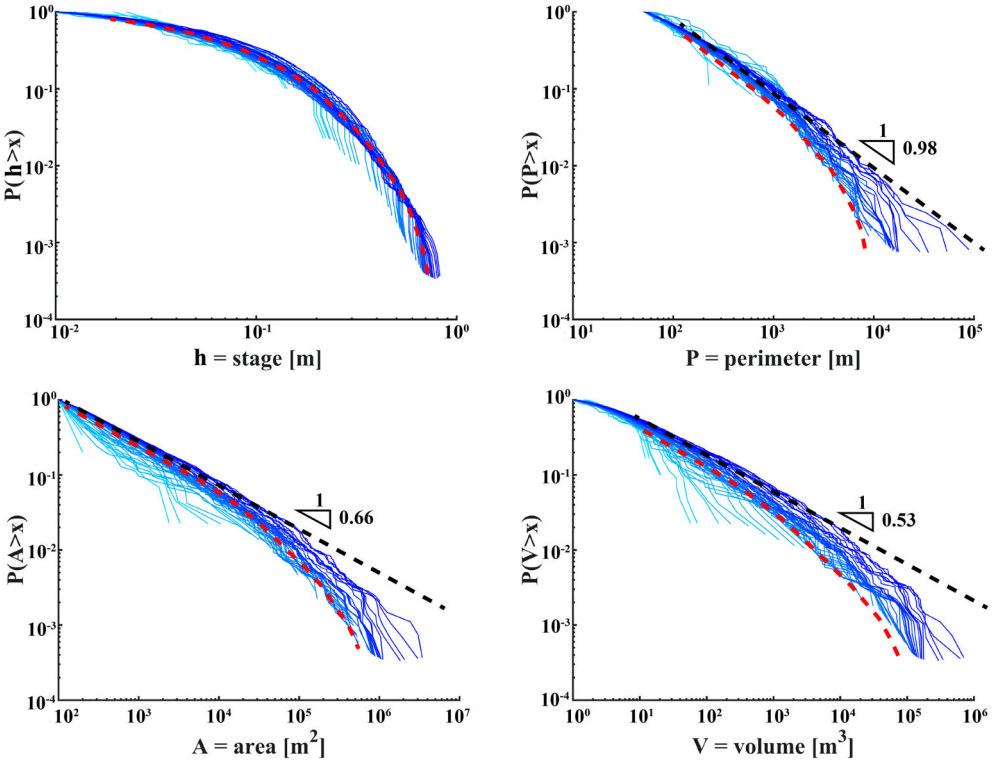

FIGURE 7 CCDFs for wetland stage, perimeter, area, and volume in the Green Swamp Area. Darker blue lines are associated with higher groundwater levels. The black dashed lines represent the scaling of the power law distribution for wetland perimeter, area, and volume. The red dashed lines indicate the lower boundary of the CCDF envelopes, characterized by a tempering constant, $c > 0$, which is, respectively, 3.58×10^{-6}, 3.28×10^{-4}, and 7.52×10^{-5} for wetland area, perimeter, and volume distributions. The scaling exponent b of the exponentially tempered Pareto distribution is reported above the dashed line in each plot. CCDF, complementary cumulative distribution function

results reported for other water bodies (Cael & Seekell, 2016; Downing et al., 2006; Steele & Heffernan, 2017). Tempering of the tail is related to finite size-effects (the dimension of the DEM limits the maximum size of wetlands) or variation in the hydro-climatic forcing (Liu & Schwartz, 2011; B. Zhang et al., 2009). The distributions of such objects have been found to follow Pareto distributions, consistent with Figure 7c. As stated in Section 2.4, the scaling exponent, b, of the wetland area distribution is related to wetlandscape fractal dimension as $D = 2b$ (Russ, 1994; Seekell et al., 2013). For the Green Swamp wetlandscape $b = 0.66 \pm 0.02$, and, thus $D = 1.32 \pm 0.04$. This estimate is supported by the comparison with the value determined based on the relationship between wetland perimeter, P, and area, A (see Supporting Information), which gives $D = 1.30 \pm 0.05$. This result suggests that the Green Swamp wetlandscape is mainly characterized by a limited degree of complexity for wetland shapes.

5 | DISCUSSION

5.1 | Limitations of minimalist approach

We proposed a minimalist approach to evaluate the temporal variability in the number of inundated wetlands based on: (a) DEM data to identify depressions where water can accumulate, and (b) thresholds of shallow groundwater level parallel to the mean slope of the terrain. As the shallow groundwater rises/falls, the filling and merging of potential wetlands are governed by the landscape topography (Chu, 2017), described here by the statistical distributions of the wetland bottoms and divides. The proposed model may not be applicable when wetland hydrology is mainly driven by precipitation or surface runoff (Leibowitz, Mushet, & Newton, 2016; Scheliga, Tetzlaff, Nuetzmann, & Soulsby, 2019; Shaw, Vanderkamp, Conly, Pietroniro, & Martz, 2012). Indeed, differences in water storage between uplands and inundated wetlands drive differences in water level response to hydroclimatic forcing, leading to frequent reversals in hydraulic gradient that cause wetlands to act as both groundwater sinks and sources (McLaughlin, Kaplan, & Cohen, 2014; Min, Perkins, & Jawitz, 2010). Furthermore, when local relief and vertical heterogeneities are too large, or in the presence of river networks or large lakes (Winter, 1999), the assumption of considering wetland dynamics as only driven by the fluctuations of a groundwater parallel to landscape topography is not valid.

The proposed model estimates the temporal changes in the number of inundated wetlands with shifts in shallow groundwater, and statistical distributions of several wetland attributes (stage, surface area, wetted perimeter and storage volume). While there is insufficient monitoring data for direct comparison with our model, we use the NWI database as a surrogate that represents an aggregation over

multiple temporal scales of wetland presence. The NWI can thus be considered a proxy for the estimation of the maximum number of inundated wetlands. The NWI estimates the presence of almost 1,300 wetlands, impressively close to the maximum number of inundated wetlands prescribed by our model N_a= 1,500. Differences between these values could be related to well-documented limitations of the NWI (Tiner, 1997), with omission errors underrepresenting small wetlands. Also, not all the wetlands identified by the proposed model are necessarily actual wetlands in the landscape. For example, we can identify landscape depressions as potential wetlands even if they cannot support hydrophytes. In addition, some of the inundated wetlands identified by the groundwater-dominated model could be DEM artefacts that do not represent actual features of the landscape (Lindsay & Creed, 2006).

The resolution and the quality of the DEM is a possible limitation of our proposed method, since it could limit the ability to correctly define the wetland bottom and divide elevations. Overall, the comparison suggests that the minimalist model proposed in this paper is able to reliably represent the number of wetlands distributed in the GSA. Remote sensing techniques using multi-temporal satellite images may represent a possible solution in future work to detect the spatiotemporal changes in inundation patterns at landscape scale (Montgomery et al., 2018; Wu & Lane, 2017; B. Zhang et al., 2009), and the advances in high resolution Lidar-based surveying may help in removing errors associated with coarser DEMs.

5.2 | Emergent wetlandscape behaviour

The geometrical features obtained when a horizontal plane (e.g., shallow groundwater) intersects a self-affine fractal surface (e.g., detrended topography) are also fractal (Russ, 1994). The direct analogy of this approach is to measure the areas of the objects (e.g., islands, lakes, and wetlands) that lie below the xy-plane (Seekell et al., 2013). The tempering constant, c, that characterizes the CCDFs of wetlands attributes (Figure 7) reflects the hydroclimatic controls on groundwater level and thus the wetland attribute fluctuations over time. The observed tempering is also induced by the finite-size effect that limits the expected power law scaling in wetlands surface area, perimeter, and volume.

The emergent scaling relationships for wetland area, storage volume and wetted perimeter distributions indicate that smaller wetlands have a disproportionate impact on open surface area and water storage volume in wetlandscapes (Shook et al., 2013; B. Zhang et al., 2009), highlighting the importance of the often overlooked and poorly identified small waterbodies (Downing, 2010). The emergent fractality in wetlandscapes is related to the self-affinity property of topographic surfaces. We argue that the self-affinity that characterizes landscape topography is translated into the spatial arrangement and the fractal geometry of wetlands. The proposed probabilistic approach (Figure 6b, d) links the number of inundated wetlands to key statistical properties of the wetlandscape, which are less sensitive to the specific choice of the size and position of the simulated domain and, therefore, more suited to extrapolate information across scales within individual landscapes. The distributions of wetland bottom and divide were similar for landscapes of different sizes (3 km × 3 km, 5 km × 5 km, 10 km × 10 km, and 20 km × 20 km) and, thus the fraction of inundated wetlands as function of groundwater level.

5.3 | Implications

The strength of the probabilistic model, expressed in Equation (5), is in its generality. The generalized dynamics of filling, merging and splitting could be extended to include an additional degree of complexity by considering the soil properties at the bottom of each potential wetland. The heterogeneities in wetland permeability could be translated in temporal lags factor during filling and draining processes. This could be viewed as simply shifting wetland bottom elevation, causing a delay in wetland filling or draining in comparison to the groundwater table. However, to implement this process it would be necessary to know the soil properties of the landscape, as well as coupled groundwater and wetland data for all the considered wetlands.

Our approach can be used to assess how the variations in the groundwater, driven by long-term fluctuations in the hydroclimatic forcing, would impact the distribution of the number of inundated wetlands in a given landscape. The impact of the shallow groundwater on the number of inundated wetlands in the GSA is evident in Figure 6b. The hydrologic dynamics of these waterbodies are extremely sensitive to water table variability. Indeed, if the shallow groundwater is lowered either from climate change or anthropogenic withdrawals, the landscape would only sustain a limited number of inundated wetlands and thus endangering ecosystem resilience. This is of key importance for the conservation of water resources not only in the GSA (Lee, 2009; Metz, 2011), but more generally for a wide range of eco-hydrological services provided by surface-subsurface water connectivity between wetlands and their surrounding uplands (McLaughlin & Cohen, 2013). Surface and subsurface storage and connectivity among individual wetlands controls the diversity of pond permanence within a wetlandscape, resulting in a variety of eco-hydrological functionalities necessary for maintaining the integrity of these ecosystems.

The proposed parsimonious model generates the spatiotemporal hydrologic dynamics of wetlandscapes in which all wetlands respond to the temporal variability of the shallow groundwater. The water table dynamics are in turn induced by stochastic hydroclimatic forcing (precipitation patterns and potential evapotranspiration). Understanding the impacts of these dynamics on the distribution of the inundated wetlands (f_{aw}) could reveal important eco-hydrological implications. Wetlands are discrete patches in heterogeneous landscapes, and act as aquatic habitat patches and node in ecological corridors to favour the dispersal of species across the region. Indeed, aquatic habitat connectivity facilitates animal dispersal, genetic flow, and multiple other ecological functions of a landscape (Ricotta, 2000), and is essential for wildlife population survival (Fahrig & Merriam, 1994) and reduction of extinction risk (Kramer-Schadt, Revilla, Wiegand, & Breitenmoser, 2004). For example, considering potential dispersal of aquatic and

semi-aquatic species during 'wet' conditions for which f_{aw} is maximized (e.g., $z_{gw} = z_C$), the species can explore a large number of diverse wetlands as habitats.

Climate and landscape spatial configuration are the two major environmental drivers of patch habitat connectivity. Seasonally wet conditions can facilitate movement of organisms through temporary surface flow or reduced separation distance among wetted habitats. In contrast, during dry conditions seasonal wetlands might not fill at all, and motivating organisms to move to alternate aquatic habitats within their dispersal distance range. Thus, examining how wetlandscapes respond to the variability in hydroclimatic forcing represents an essential step to characterize the variations in spatiotemporal connectivity and occupancy at landscape scales, which is important for species that rely on these transitional habitats for their dispersal and survival.

6 | CONCLUSIONS

Wetlands are a product of landscape geologic, geomorphic, and hydrologic history. The overall physical structure and hydrology of wetlands is determined by the interplay between geomorphological and climatic factors. Here, we proposed a wetland modelling approach that uses DEM data and specified thresholds of shallow groundwater level to evaluate the spatiotemporal hydrologic dynamics of wetlandscapes. We evaluated the model with DEM and hydrologic data from the Green Swamp Area, Florida, a landscape characterized by many isolated wetlands. We used detailed data from six cypress-dome wetlands and found that the hydrologic dynamics are strongly influenced by the fluctuations of the shallow groundwater. Our analyses suggest that coupling of groundwater and landscape topography is sufficient to identify the locations and spatial extent of wetlands at the landscape scale. We also estimated the temporal changes in the number of inundated wetlands as a function of groundwater level, and their statistical distributions in terms of stage, surface area, wetted perimeter, and storage volume. Recognizing how the interplay between landscape topography and hydrology causes variability in wetland morphological and habitat attributes allows for characterization of the spatial pattern of ecological connectivity among dynamic patchy habitats.

ACKNOWLEDGEMENTS

Lee A. Reith Endowment in the Lyles School of Civil Engineering at Purdue University provided partial financial support for this research. PSCR acknowledges support from two National Science Foundation (NSF) grants: NSF Collaboration Research, RIPS Type 2: Resilience simulation for water, power, and road networks, Award# 1441188; NSF Award# 1354900, 'Plant adaptation in variable environments'.

CONFLICT OF INTEREST

The authors have no conflict of interest to declare.

DATA AVAILABILITY STATEMENT

The data that support the findings of this study are publicly available. Data for wetlands and groundwater level can be found at the SWFWMD website. Data for wetland extent are available at the National Wetland Inventory website, while the DEM was obtained from National Map Viewer website. All our analyses were conducted using Matlab R2016b.

ORCID

Leonardo E. Bertassello https://orcid.org/0000-0001-5168-2142
P. Suresh C. Rao https://orcid.org/0000-0002-5982-3736
James W. Jawitz https://orcid.org/0000-0002-6745-0765
Antoine F. Aubeneau https://orcid.org/0000-0001-8373-9342
Gianluca Botter https://orcid.org/0000-0003-0576-8847

REFERENCES

Acharya, S., Jawitz, J. W., & Mylavarapu, R. S. (2012). Analytical expressions for drainable and fillable porosity of phreatic aquifers under vertical fluxes from evapotranspiration and recharge. *Water Resources Research*, *48*, W11526. https://doi.org/10.1029/2012WR012043

Bertassello, L. E., Rao, P. S. C., Jawitz, J. W., Botter, G., Le, P. V. V., Kumar, P., & Aubeneau, A. F. (2018). Wetlandscape fractal topography. *Geophysical Research Letters*, *45*, 6983–6991. https://doi.org/10.1029/2018GL079094

Bertassello, L. E., Rao, P. S. C., Park, J., Jawitz, J. W., & Botter, G. (2018). Stochastic modeling of wetland-groundwater systems. *Advances in Water Resources*, *112*, 214–223.

Botter, G., Basso, S., Rodriguez-Iturbe, I., & Rinaldo, A. (2013). Resilience of river flow regimes. *Proceedings of the National Academy of Sciences of the United States of America*, *110*(32), 12925–12930. https://doi.org/10.1073/pnas.1311920110

Cael, B. B., & Seekell, D. A. (2016). The size-distribution of Earth's lakes. *Scientific Reports*, *6*, 29633. https://doi.org/10.1038/srep29633

Cheng, F. Y., & Basu, N. B. (2017). Biogeochemical hotspots: Role of small water bodies in landscape nutrient processing. *Water Resource Research*, *53*, 5038–5056. https://doi.org/10.1002/2016WR020102

Chu, X. (2017). Delineation of pothole-dominated wetlands and modeling of their threshold behaviors. *Journal of Hydrologic Engineering*, *22*(1), 1–11. https://doi.org/10.1061/(ASCE)HE.1943-5584.0001224

Chu, X., Zhang, J., Chi, Y., & Yang, J. (2010). An improved method for watershed delineation and computation of surface depression storage. In K. W. Potter, & D. K. Frevert (Eds.), *Watershed management 2010: Innovations in watershed management under land use and climate change, Chap. 99* (pp. 1113–1122). Reston, VA: American Society of Civil Engineers. https://doi.org/10.1061/41143(394)100

Cohen, M. J., Creed, I. F., Alexander, L., Basu, N. B., Calhoun, A. J., Craft, C., D'Amico E., DeKeyser E., Fowler L., Golden H.E., Jawitz, J. W., Kalla P., Kirkman L.K., Lane C.R., Lanf M., Leibowitz S.G. Lewis D.B., Marton J., McLaughlin D L, Musget D.M., Raanan-Kiperwas H., Rains M.C., Smith L., and Walls S.C. (2016). *Do geographically isolated wetlands influence landscape functions? Proceedings of the National Academy of Sciences*, *113*, *1978–1986*, doi:https://doi.org/10.1073/pnas.1512650113.

Cronk, J. K., & Fennessy, M. S. (2016). *Wetland plants: Biology and ecology*. CRC press.

Downing, J. A. (2010). Emerging global role of small lakes and ponds: Little things mean a lot. *Limnetica*, *29*, 9–24.

Downing, J. A., Prairie, Y. T., Cole, J. J., Duarte, C. M., Tranvik, L. J., Striegl, R. G., … Middelburg, J. J. (2006). The global abundance and size distribution of lakes, ponds, and impoundments. *Limnology and Oceanography*, *51*. https://doi.org/10.4319/lo.2006.51.5.2388

Ewel, K. C. (1990). Multiple demands on wetlands. *Bioscience*, *40*(9), 660–666.

Fahrig, L., & Merriam, G. (1994). Conservation of fragmented populations. *Conservation Biology*, *8*(1), 50–59.

Haag, K.H., & Lee, T.M. (2010). *Hydrology and ecology of freshwater wetlands in Central Florida—A primer*. U.S. Geological Survey Circular, 1342, p. 138.

Haag, K. H., Lee, T. M., & Herndon, D. C. (2005). *Bathymetry and vegetation in isolated marsh and cypress wetlands in the Northern Tampa Bay Area, 2000-2004*. U.S. Geological Survey Scientific Investigations Report 2005-5109, p. 49.

Huang, S., Young, C., Feng, M., Heidemann, K., Cushing, M., Mushet, D. M., & Liu, S. (2011). Demonstration of a conceptual model for using LiDAR to improve the estimation of floodwater mitigation potential of Prairie Pothole Region wetlands. *Journal of Hydrology*, *405* (3–4), 417–426. https://doi.org/10.1016/j.jhydrol.2011.05.040

Jaramillo, F., Brown, I., Castellazzi, P., Espinosa, L., Guittard, A., Hong, S. H., … Wdowinski, S. (2018). Assessment of hydrologic connectivity in an ungauged wetland with InSAR observations. *Environmental Research Letters*, *13*(2), 024003.

Kramer-Schadt, S., Revilla, E., Wiegand, T., & Breitenmoser, U. R. S. (2004). Fragmented landscapes, road mortality and patch connectivity: Modelling influences on the dispersal of Eurasian lynx. *Journal of Applied Ecology*, *41*(4), 711–723.

Le, P. V. V., & Kumar, P. (2014). Power law scaling of topographic depressions and their hydrologic connectivity. *Geophysical Research Letters*, *41*, 1553–1559. https://doi.org/10.1002/2013GL059114

Lee, T. M. (2009). *Comparative hydrology, water quality, and ecology of selected natural and augmented freshwater wetlands in west-Central Florida*. (Report No. 1758). US Geological Survey.

Leibowitz, S. G. (2003). Isolated wetlands and their functions: An ecological perspective. *Wetlands*, *23*(3), 517–531.

Leibowitz, S. G., Mushet, D. M., & Newton, W. E. (2016). Intermittent surface water connectivity: Fill and spill vs. fill and merge dynamics. *Wetlands*, *36*(S2), 323–342. https://doi.org/10.1007/s13157-016-0830-z

Lindsay, J. B., & Creed, I. F. (2006). Distinguishing actual and artefact depressions in digital elevation data. *Computers & Geosciences*, *32*(8), 1192–1204.

Liu, G., & Schwartz, F. W. (2011). An integrated observational and model-based analysis of the hydrologic response of prairie pothole systems to variability in climate. *Water Resources Research*, *47*(2).

McLaughlin, D. L., & Cohen, M. J. (2013). Realizing ecosystem services: Wetland hydrologic function along a gradient of ecosystem condition. *Ecological Applications*, *23*(7), 1619–1631.

McLaughlin, D. L., Diamond, J. S., Quintero, C., Heffernan, J., & Cohen, M. J. (2019). Wetland connectivity thresholds and flow dynamics from stage measurements. *Water Resources Research*, *55*(7), 6018–6032.

McLaughlin, D. L., Kaplan, D. A., & Cohen, M. J. (2014). A significant nexus: Geographically isolated wetlands influence landscape hydrology. *Water Resources Research*, *50*(9), 7153–7166.

Metz, P. A. (2011). *Factors that influence the hydrologic recovery of wetlands in the Northern Tampa Bay area, Florida*. US Department of the Interior, US Geological Survey.

Min, J. H., Paudel, R., & Jawitz, J. W. (2010). Spatially distributed modeling of surface water flow dynamics in the everglades ridge and slough landscape. *Journal of Hydrology*, *390*, 1–12. https://doi.org/10.1016/j.jhydrol.2010.06.023

Min, J. H., Perkins, D. B., & Jawitz, J. W. (2010). Wetland-groundwater interactions in subtropical depressional wetlands. *Wetlands*, *30*(5), 997–1006.

Mitsch, W. J., & Gosselink, J. G. (2015). *Wetlands* (5th ed.). New York, NY: John Wiley & Sons.

Montgomery, J. S., Hopkinson, C., Brisco, B., Patterson, S., & Rood, S. B. (2018). Wetland hydroperiod classification in the western prairies using multitemporal synthetic aperture radar. *Hydrological Processes*, *32*(10), 1476–1490.

Mushet, D. M., Alexander, L. C., Bennett, M., Schofield, K., Christensen, J. R., Ali, G., … Lang, M. W. (2019). Differing modes of biotic connectivity within freshwater ecosystem mosaics. *JAWRA Journal of the American Water Resources Association*, *55*(2), 307–317.

National Map Viewer. (n.d.). Available at https://viewer.nationalmap.gov

National Wetland Inventory. (n.d.). Available at https://www.fws.gov/wetlands

Nilsson, K. A., Rains, M. C., Lewis, D. B., & Trout, K. E. (2013). Hydrologic characterization of 56 geographically isolated wetlands in west-Central Florida using a probabilistic method. *Wetlands Ecology and Management*, *21*(1), 1–14. https://doi.org/10.1007/s11273-012-9275-1

Osher, S., & Fedkiw, R. P. (2001). Level set methods: An overview and some recent results. *Journal of Computational Physics*, *169*(2), 463–502.

Park, J., Botter, G., Jawitz, J. W., & Rao, P. S. C. (2014). Stochastic modeling of hydrologic variability of geographically isolated wetlands: Effects of hydro-climatic forcing and wetland bathymetry. *Advances in Water Resources*, *69*, 38–48. https://doi.org/10.1016/j.advwatres.2014.03.007

Peters, D. P., Groffman, P. M., Nadelhoffer, K. J., Grimm, N. B., Collins, S. L., Michener, W. K., & Huston, M. A. (2008). Living in an increasingly connected world: A framework for continental-scale environmental science. *Frontiers in Ecology and the Environment*, *6*(5), 229–237.

Porporato, A., Daly, E., & Rodriguez-Iturbe, I. (2004). Soil water balance and ecosystem response to climate change. *The American Naturalist*, *164*(5), 625–632. https://doi.org/10.1086/424970

Powell, K. M., Wynn, J. G., Rains, M. C., Stewart, M. T., & Emery, S. (2019). Soil indicators of hydrologic health and resilience in cypress domes of West-Central Florida. *Ecological Indicators*, *97*, 269–279.

Pride, R. W., Meyer, F. W., & Cherry, R. N. (1961). *Interim report on the hydrologic features of the green swamp area in Central Florida*.

Rains, M. . C., Leibowitz, S. . G., Cohen, M. . J., Creed, I. . F., Golden, H. . E., Jawitz, J. W., … McLaughlin, D. L. (2016). Geographically isolated wetlands are part of the hydrological landscape. *Hydrological Processes*, *30*, 153–160. https://doi.org/10.1002/hyp.10610

Ricotta, C. (2000). From theoretical ecology to statistical physics and back: Self-similar landscape metrics as a synthesis of ecological diversity and geometrical complexity. *Ecological Modelling*, *125*(2–3), 245–253.

Rochow, T.F., & M. Lopez. 1984. *Hydrobiological monitoring of cypress domes in the Green Swamp area of Lake and Sumter counties, Florida 1979–1982*. Environmental Section Technical Report 1984-1. Southwest Florida Water Management District. p. 79.

Russ, J. C. (1994). *Fractal surfaces*. New York, NY: Plenum.

Scheliga, B., Tetzlaff, D., Nuetzmann, G., & Soulsby, C. (2019). Assessing runoff generation in riparian wetlands: Monitoring groundwater–surface water dynamics at the micro-catchment scale. *Environmental Monitoring and Assessment*, *191*(2), 116.

Seekell, D. A., & Pace, M. L. (2011). Does the Pareto distribution adequately describe the size-distribution of lakes? *Limnology and Oceanography*, *56*(1), 350–356.

Seekell, D. A., Pace, M. L., Tranvik, L. J., & Verpoorter, C. (2013). A fractal-based approach to lake size-distributions. *Geophysical Research Letters*, *40*, 517–521. https://doi.org/10.1002/grl.50139

Shaw, D. A., Vanderkamp, G., Conly, F. M., Pietroniro, A., & Martz, L. (2012). The fill–spill hydrology of prairie wetland complexes during drought and deluge. *Hydrological Processes*, *26*(20), 3147–3156.

Shook, K., Pomeroy, J. W., Spence, C., & Boychuk, L. (2013). Storage dynamics simulations in prairie wetland hydrology models: Evaluation and parameterization. *Hydrological Processes*, *27*, 1875–1889. https://doi.org/10.1002/hyp.986

Smith, A., Tetzlaff, D., Gelbrecht, J., Kleine, L., & Soulsby, C. (2019). Riparian wetland rehabilitation and beaver re-colonization impacts on hydrological processes and water quality in a lowland agricultural catchment. *Science of the Total Environment*, *134302*.

Sophocleous, M. (2002). Interactions between groundwater and surface water: The state of the science. *Hydrogeology Journal*, *10*(1), 52–67.

Spechler, R. M., & Kroening, S. E. (2007). *Hydrology of Polk County, Florida*. U.S. Geological Survey Scientific Investigations Report 2006-5320, p. 114.

Steele, M. K., & Heffernan, J. B. (2017). Land use and topography bend and break fractal rules of water body size-distributions. *Limnology and Oceanography Letters*, *2*(3), 71–80.

Tamea, S., Muneepeerakul, R., Laio, F., Ridolfi, L., & Rodriguez-Iturbe, I. (2010). Stochastic description of water table fluctuations in wetlands. *Geophysical Research Letters*, *37*(6).

Tetzlaff, D., Soulsby, C., Bacon, P. J., Youngson, A. F., Gibbins, C., & Malcolm, I. A. (2007). Connectivity between landscapes and riverscapes—A unifying theme in integrating hydrology and ecology in catchment science? *Hydrological Processes: An International Journal*, *21* (10), 1385–1389.

Thorslund, J., Jarsjo, J., Jaramillo, F., Jawitz, J. W., Manzoni, S., Basu, N. B., … Hylin, A. (2017). Wetlands as large-scale nature-based solutions: Status and challenges for research, engineering and management. *Ecological Engineering*, *108*, 489–497.

Tiner, R. W. (1997). NWI maps: What they tell us. *National Wetlands Newsletter*, *19*(2), 7–12.

Tiner, R. W. (2016). *Wetland indicators: A guide to wetland formation, identification, delineation, classification, and mapping* (2nd ed.). CRC Press. ISBN: 9781439853702.

Tóth, J. Ó. Z. S. E. F. (1962). A theory of groundwater motion in small drainage basins in Central Alberta, Canada. *Journal of Geophysical Research*, *67*(11), 4375–4388.

Uden, D. R., Hellman, M. L., Angeler, D. G., & Allen, C. R. (2014). The role of reserves and anthropogenic habitats for functional connectivity and resilience of ephemeral wetlands. *Ecological Applications*, *24*(7), 1569–1582.

Werner, E. E., Skelly, D. K., Relyea, R. A., & Yurewicz, K. L. (2007). Amphibian species richness across environmental gradients. *Oikos*, *116*, 1697–1712. https://doi.org/10.1111/j.0030-1299

Winter, T. C. (1999). Relation of streams, lakes, and wetlands to groundwater flow systems. *Hydrogeology Journal*, *7*(1), 28–45. https://doi.org/10.1007/s100400050178

Wu, Q., & Lane, C. R. (2017). Delineating wetland catchments and modeling hydrologic connectivity using lidar data and aerial imagery. *Hydrology and Earth System Sciences*, *21*, 3579–3595. https://doi.org/10.5194/hess-21-3579-2017

Wu, Q., Lane, C. R., Wang, L., Vanderhoof, M. K., Christensen, J. R., & Liu, H. (2019). Efficient delineation of nested depression hierarchy in digital elevation models for hydrological analysis using level-set method. *JAWRA Journal of the American Water Resources Association*, *55*(2), 354–368.

Zhang, B., Schwartz, F. W., & Liu, G. (2009). Systematics in the size structure of prairie pothole lakes through drought and deluge. *Water Resource Research*, *45*, W04421. https://doi.org/10.1029/2008WR006878

Zhang, Y., Cui, B., Lan, Y., Han, Z., Wang, T., & Guo, A. (2012). Four terrestrialization characteristics of Baiyangdian Lake, China. *Procedia Environmental Sciences*, *13*, 645–654.

SUPPORTING INFORMATION

Additional supporting information may be found online in the Supporting Information section at the end of this article.

How to cite this article: Bertassello LE, Rao PSC, Jawitz JW, Aubeneau AF, Botter G. Wetlandscape hydrologic dynamics driven by shallow groundwater and landscape topography. *Hydrological Processes*. 2019;1–15. https://doi.org/10.1002/hyp.13661